Available online at www.sciencedirect.com
SCIENCE DIRECT®
Infrared Physics & Technology 47 (2006) 227–239
INFRARED PHYSICS & TECHNOLOGY
www.elsevier.com/locate/infrared

# Intensities of line features in vibration-rotational bands 2–0 to 6–0 of $^{14}N^{16}O$ $X^2\Pi_r$ and experimental evaluation of a radial function for electric dipolar moment

Yuan-Pern Lee [a,b], Swee-Lan Cheah [c], J.F. Ogilvie [d,*]

[a] *Department of Applied Chemistry and Institute of Molecular Science, National Chiao Tung University, 1001 Ta-Hsueh Road, Hsinchu 30010, Taiwan*
[b] *Institute of Atomic and Molecular Sciences, Academia Sinica, Taipei 106, Taiwan*
[c] *Department of Chemistry, National Tsing Hua University, 101, Section 2, Kuang Fu Road, Hsinchu 30013, Taiwan*
[d] *Escuela de Quimica, Universidad de Costa Rica, Ciudad Universitaria Rodrigo Facio, San Pedro de Montes de Oca, San Jose 2060, Costa Rica*

Received 14 September 2004
Available online 25 March 2005

**Abstract**

We measured the strengths of individual line-like features, representing unresolved Λ doublets, in vibration-rotational bands 2–0 to 6–0 of $^{14}N^{16}O$ within each substate of electronic ground state $X^2\Pi_{1/2,3/2}$ in mid and near infrared regions. Analyses of these data to derive values of matrix elements for vibrational transitions enabled production of a radial function for electric dipolar moment, containing seven parameters, that satisfactorily reproduces the intensities of about 700 such features for vibrational states up to $v = 6$.


## 1. Introduction

We have measured the intensities of individual features in vibration-rotational bands of gaseous NO near 300 K from the first to the fifth overtone, or to vibrational states $v' = 2$, 3, 4, 5 and 6 from $v'' = 0$. Each such band within the electronic ground state $X^2\Pi_{1/2,3/2}$ has 24 branches, but 12 of these occur in two somewhat separate satellite bands, which involve also a change of total electronic angular momentum between electronic substates, and of which their consequent weakness makes them generally difficult to detect. Because our spectral resolution was insufficient to separate the Λ doublets, we observed effectively six branches of line-like features, comprising two weak Q

* Corresponding author.
*E-mail addresses:* yplee@mail.nctu.edu.tw (Y.-P. Lee), ogilvie@cecm.sfu.ca (J.F. Ogilvie).

1350-4495/$ - see front matter © 2005 Elsevier B.V. All rights reserved.
doi:10.1016/j.infrared.2005.01.002

branches near the centre of each band and two intense P and R branches on each side of that centre. For each of five specified bands we measured the strengths of these features and present here the results of our analysis of these intensity data; this analysis yields a radial function, i.e. of internuclear distance $R$, of electric dipolar moment $p(R)$ that reproduces those data within experimental uncertainties of measurement, which we compare with calculated data.

Previously reported measurements [1–3] of intensities of vibration-rotational bands of NO were based on gross features as a result of broadening through use of gaseous samples at large pressures, with these pertinent exceptions: there exist two independent measurements [4,5] of individual lines or features in the fundamental band, 1–0, two separate measurements of individual lines in the first overtone [6,7], 2–0, and single measurements of a band originating in $v'' = 1$ in the sequence with $\Delta v = 1$, or band 2–1 [8], and a band originating in $v'' = 1$ in the sequence with $\Delta v = 2$, or band 3–1 [9], with our own previous work on bands 5–0 [10] and 6–0 [11]. We have reanalysed the latter spectra, and here combine those data with fresh measurements on bands 2–0, 3–0 and 4–0 in a consistent manner to derive $p(R)$ according to an established method [12].

## 2. Experiments

We recorded all spectra with an interferometric spectrometer (Bomem DA8, evacuated to $\sim$15 N m$^{-2}$) and a large vessel to contain gaseous samples. The latter cylindrical cell (Infrared Associates, model 100, of White type) has an optical path of length 1.375 m between mirrors for multiple internal reflections to produce an optical path variable between 8.25 m and 107.25 m in increments 11 m. Spots in sequences on internal mirrors from the beam of a helium-neon laser enable a precise count of a number of passes of the beam through a gaseous sample. The number of passes that we employ depends on the band being measured and the pressure of NO required to yield maximum net absorbance, $\log_{10}(I_0/I)$, of the most intense feature in each band less than $\sim$0.12, to avoid distortion of signals from effects of saturation. With a capacitance manometer (MKS model 122A, precision 0.5% of reading), we measured the pressure of a gaseous sample before and after each collection of interferograms. We employed partial pressures (N m$^{-2}$) of NO in a range [68, $1.07 \times 10^5$] as appropriate for a particular band, within the limitations of properties of the cell; with NO at small partial pressures we added He gas to a total pressure at least 67,000 N m$^{-2}$ to ensure broadening of lines to widths substantially greater than the spectral resolution. We recorded interferograms for samples generally at three pressures, with at least two separate collections at each pressure. With two digital thermometers (Omega, thermocouples of type K) that indicate maximum and minimum temperatures (in °C) over a duration of spectral measurements, we monitored the temperature of the vessel at each end; for all spectra accepted for analysis here, the maximum variation was ±0.5 K about the mean.

To obtain the best conditions for each band, for spectral measurements we employed beam splitters made of $CaF_2$ for band 2–0 and of quartz for bands 3–0 to 6–0, a SiC or tungsten filament as source, and an InSb detector near 77 K or a Si photodiode at ambient temperature. To limit the spectral region of radiation reaching a detector, we selected optical filters (CVI, Optical Coatings Limited, Omega, and Spectrogon) to provide pass bands about the band of intended measurement. Optical resolution was set at 1.0 or 1.5, 1.3 or 1.5, 4.0, 6.0 and 6.0 m$^{-1}$ for bands 2, 3, 4, 5, 6–0, respectively, which was appreciably smaller than the apparent width of isolated individual spectral features in each case. We co-added interferograms numbering 300–750 and accumulated over periods up to 13.5 h. A ratio of a spectrum from each co-added interferogram with a reference spectrum yielded an absorbance spectrum, of which a sample for band 4–0 appears in Fig. 1. To reduce these spectra, and for further analysis of data, we employed software (Grams, Galactic Industries) designed to operate with the interferometric spectrometer; the characteristics (wave number, stature or apparent maximum net absorbance, width and area) of each feature were collected into a commercial spreadsheet, and further calculations

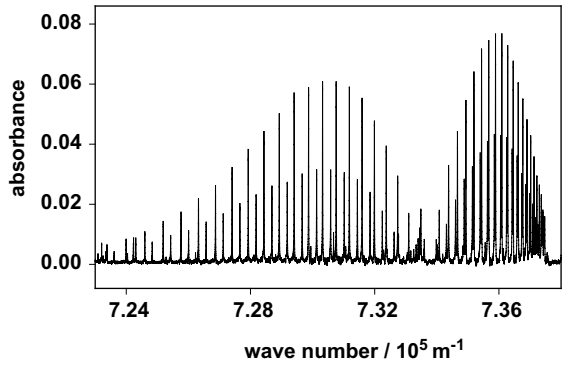


Fig. 1. Spectrum of band 4–0 of gaseous $^{14}N^{16}O$ at pressure 73,300 N m$^{-2}$ and 298 K with length 8.25 m of absorbing path and spectral resolution 4.0 m$^{-1}$.

were conducted with a symbolic processor (Maple 9.5, Maplesoft, Waterloo Maple Inc.). Strengths of more intense lines in each band have uncertainties ~10%, but for weak lines up to 30%; statistical weights based on multiple spectra were applied in spectral reduction.

To purify gaseous NO (AGA Specialty Gas, nominal chemical purity 99.5% in a cylinder as received), we passed the gas slowly through a trap charged with silica gel and cooled below 195 K [13]; this treatment served to diminish greatly other oxides of nitrogen, but not $N_2$. Tests of purity based on spectra in the mid infrared region indicated that remaining impurities occurred at a negligible level. Because the vessel has a large volume and large area of internal surface, its evacuation through a narrow valve presented a problem for removal of residual water vapour, notorious for its retention on polar or metallic surfaces. In the regions of bands 2–0, 3–0, 4–0 and 6–0 of NO, vestigial water vapour either in the vessel or within the optical path inside the interferometer can absorb intensely, as transitions of $H_2O$ involve fewer vibrational quanta than for NO in the same region. For this reason, to achieve minimal interference from spectral lines of $H_2O$ at wave numbers of lines of NO, protracted pumping of both the vessel and the space inside the interferometer is essential. Comparison of Fig. 1 with a published spectrum [14] for band 4–0 of NO indicates the extent of our success. Under our conditions of preparation for recording of spectra and our fitting of all lines within each selected short segment of wave number scale, and in the absence of fortuitous coincidences between intense lines of $H_2O$ and of NO, interference from $H_2O$ with our measurements of spectral features of NO is generally negligible.

## 3. Theoretical basis

For absorption by a diatomic molecular species in electronic state $X\,^1\Sigma$ within a gaseous sample at temperature $T$, the strength $S_l$ of a line attributed to a spectral transition from a state $|0, J''\rangle$ to another state $|v', J'\rangle$ in a vibration-rotational spectrum is represented according to [12]

$$S_l = (8\pi^3/3hc)[\exp(-hcE_{0J}/k_BT)/4\pi\epsilon_0 Q]\tilde{\nu}_0 \times [1-\exp(-hc\tilde{\nu}_0/k_BT)]|\imath||\langle v'J'|p(x)|0,J''\rangle|^2 \quad (1)$$

in which appear fundamental physical constants $h$, $c$, $k_B$ and $\epsilon_0$, total partition function $Q$, spectral term $E_{0J}$ of the initial state $|0, J''\rangle$ of a transition, and wave number $\tilde{\nu}_0$ of the transition; $\imath \equiv 1/2[J'(J'+1) - J''(J''+1)]$ is a running number of value $J''+1$ for a line in branch R or $-J''$ for a line in branch P. In $|\langle v'J'p(x)|0, J''\rangle|^2$ that is a square of an experimental matrix element for a transition between specified states, $p(x)$ is a radial function for electric dipolar moment of an absorbing molecular species in terms of reduced displacement $x = (R - R_e)/R_e$ with internuclear distances instantaneous $R$ and equilibrium $R_e$. Modification of this formula to make it applicable to a molecule such as NO in an electronic state $^2\Pi_r$ with small coupling between electronic spin and orbital angular momenta requires taking into account that the total partition function $Q$ includes rotational states in the vibrational ground state of the electronic ground state $^2\Pi_{1/2}$ but also in the vibrational ground state of electronic state $^2\Pi_{3/2}$ lying above $^2\Pi_{1/2}$ by only 12313.361 m$^{-1}$ [15], and a vibrational factor ~1, with a factor 2 for $\Lambda$ doubling. We calculated $Q_{rot}$ by direct summation over rotational states [15] up to $J = 40.5$ at each temperature. For application of formula (1) to NO in electronic state $^2\Pi_r$, $|\imath|$ also becomes replaced by

either $(|\imath|^2 - \Omega^2)/|\imath|$ for transitions with $\Delta J = \pm 1$ or $\Omega^2(2J+1)/[J(J+1)]$ for $\Delta J = 0$ [5]. The rotational dependence remains factorable according to [12],

$$\langle v'J'|p(x)|0,J''\rangle^2 = \langle v'|p(x)|0\rangle^2(1 + C_0^{v'}\imath + D_0^{v'}\imath^2 + \cdots) \quad (2)$$

in which $|\langle v'|p(x)|0\rangle|^2$ is the square of the pure vibrational matrix element of electric dipolar moment; the latter quantity is coefficient to a Herman-Wallis factor [12] containing coefficients $C_0^{v'}$ and $D_0^{v'}$. According to formula (1), strengths of lines and bands are proportional to squares of matrix elements; as coefficients $C_0^{v'}$ and $D_0^{v'}$ are linearly proportional to coefficients $p_j$ in an expansion of $p(x)$ [11], we apply this information to deduce the signs of $\langle v'|p(x)|0\rangle$. A sum of measured strengths $S_l$ of all lines in a particular band,

$$S_b = \sum S_l \quad (3)$$

provides an experimental estimate of a band strength $S_b$, whereas a theoretical measure depends on the wave number $\tilde{\nu}_c$ characterising the origin of a band and the square of the pure vibrational matrix element of electric dipolar moment,

$$S_b = 8\pi^2\tilde{\nu}_c|\langle v'|p(x)|0\rangle|^2/(12hc\epsilon_0) \quad (4)$$

A line strength is derived from integrated absorbance of a particular spectral line, a known number density $N$ of molecules per unit volume in a gaseous sample at temperature $T$ and an effective length $\ell$ of optical path:

$$S_l = (1/N\ell)\int \ln[I_0(\tilde{\nu})/I(\tilde{\nu})]\mathrm{d}\tilde{\nu} \quad (5)$$

For NO under our conditions of measurement, spectral lines for vibration-rotational transitions occur in closely spaced couples due to Λ doubling, but each such couple appears as an unresolved line-like feature. We include factors two in pertinent formulae to reflect this condition, and assume equal probability of transition of each component of Λ doubling, according to precedent [5].

To represent the dependence of electric dipolar moment $p$ as a function of internuclear distance $R$ or $x$ we apply a simple polynomial [12] of order sufficient for data in a particular set:

$$p(x) = \sum_{j=0} p_j x^j \quad (6)$$

A Padé function [12] is a ratio of polynomials such that successive derivatives with respect to $x$, apart from factorial factors, agree exactly with as many coefficients $p_j$ in formula (6) as can be evaluated from available data; tests on Padé functions of various orders indicate that, because of large magnitudes of coefficients $p_j$, such a form is impractical for the present data of NO. We employ SI units throughout this work and convert published values accordingly.

## 4. Results

In Tables 1–5 we present strengths of line-like features in vibration-rotational bands $v'$–0, with $v' = 2$, 3, 4, 5 and 6, respectively; each feature is characterised by both a value of quantum number $J''$ for total angular momentum of the state of lesser energy and a wave number calculated as the difference of published spectral terms [15]. From a direct sum of these strengths $S_l$ of lines according to formula (3) for a particular band we estimated a strength of each band $S_b$. In the case of band 2–0, the resulting value was about 6 per cent less than one published value [6], but the same, within experimental error, as another published value [7], either of which might be expected to be accurate; although problems with sample handling and adsorption of NO on surfaces within the large gas cell might slightly affect our measurements of that band, our independent coincidence with the later published result supports the correctness of that value [7]. Because we used the same samples of NO for corresponding measurements of band 3–0, for which only the length of optical path varied through an increased number of passes of the light through the cell, the strength of band 3–0 is as accurate as that of band 2–0; for the same reason ratios of bands 4, 5, 6–0 are likewise accurate. With large pressures of nominally pure NO used

Table 1
Values of quantum number $J''$ for total angular momentum of the lower state of a vibration-rotational transition in band 2–0, wave number/$m^{-1}$ of each apparent line in branches P, Q and R, and line strength $S_l/10^{-23}$ m observed and calculated for $^{14}N^{16}O$ in substates of electronic ground state $X^2\Pi_r$ at 298 K

| $J$ | P($J$) | $S_{l,ob}$ | $S_{l,cal}$ | Q($J$) | $S_{l,ob}$ | $S_{l,cal}$ | R($J$) | $S_{l,ob}$ | $S_{l,cal}$ |
|---|---|---|---|---|---|---|---|---|---|
| *Sub-band 2–0 for substate $^2\Pi_{1/2}$* | | | | | | | | | |
| 0.5 | | | | 372406.7 | 0.22 | 0.247 | 372898.0 | 0.50 | 0.500 |
| 1.5 | 371905.1 | 0.48 | 0.476 | 372396.4 | 0.07 | 0.096 | 373215.2 | 0.91 | 0.886 |
| 2.5 | 371560.4 | 0.84 | 0.816 | 372379.3 | 0.04 | 0.060 | 373525.6 | 1.23 | 1.226 |
| 3.5 | 371208.9 | 1.14 | 1.093 | | | | 373829.2 | 1.55 | 1.515 |
| 4.5 | 370850.5 | 1.34 | 1.306 | | | | 374125.9 | 1.66 | 1.744 |
| 5.5 | 370485.3 | 1.49 | 1.455 | | | | 374415.6 | 1.89 | 1.906 |
| 6.5 | 370113.2 | 1.60 | 1.539 | | | | 374698.6 | 1.97 | 2.000 |
| 7.5 | 369734.2 | 1.61 | 1.563 | | | | 374974.6 | 1.90 | 2.028 |
| 8.5 | 369348.4 | 1.61 | 1.533 | | | | 375243.7 | 1.73 | 1.994 |
| 9.5 | 368955.8 | 1.52 | 1.459 | | | | 375505.9 | 1.81 | 1.906 |
| 10.5 | 368556.3 | 1.42 | 1.350 | | | | 375761.1 | 1.66 | 1.780 |
| 11.5 | 368149.9 | 1.28 | 1.219 | | | | 376009.5 | 1.49 | 1.621 |
| 12.5 | 367736.7 | 1.16 | 1.074 | | | | 376250.8 | 1.37 | 1.443 |
| 13.5 | 367316.6 | 0.99 | 0.926 | | | | 376485.2 | 1.16 | 1.258 |
| 14.5 | 366889.6 | 0.85 | 0.781 | | | | 376712.5 | 1.00 | 1.073 |
| 15.5 | 366455.8 | 0.71 | 0.645 | | | | 376932.9 | 0.82 | 0.898 |
| 16.5 | 366015.1 | 0.57 | 0.522 | | | | 377146.2 | 0.68 | 0.736 |
| 17.5 | 365567.6 | 0.45 | 0.414 | | | | 377352.5 | 0.54 | 0.592 |
| 18.5 | 365113.3 | 0.34 | 0.322 | | | | 377551.6 | 0.44 | 0.467 |
| 19.5 | 364652.1 | 0.27 | 0.246 | | | | 377743.7 | 0.33 | 0.361 |
| 20.5 | 364184.1 | 0.21 | 0.184 | | | | 377928.6 | 0.25 | 0.275 |
| 21.5 | 363709.3 | 0.15 | 0.136 | | | | 378106.4 | 0.19 | 0.205 |
| 22.5 | 363227.6 | 0.11 | 0.098 | | | | 378277.1 | 0.12 | 0.150 |
| 23.5 | 362739.1 | 0.07 | 0.069 | | | | 378440.5 | 0.10 | 0.109 |
| 24.5 | 362243.9 | 0.09 | 0.048 | | | | 378596.8 | 0.07 | 0.077 |
| 25.5 | 361741.8 | 0.03 | 0.033 | | | | 378745.8 | 0.05 | 0.053 |
| 26.5 | 361233.0 | 0.02 | 0.022 | | | | 378887.5 | 0.04 | 0.036 |
| 27.5 | 360717.4 | 0.01 | 0.015 | | | | 379022.0 | 0.03 | 0.024 |
| 28.5 | 360195.0 | 0.01 | 0.010 | | | | 379149.1 | 0.02 | 0.016 |
| 29.5 | | | | | | | 379269.0 | 0.01 | 0.010 |
| 30.5 | | | | | | | 379381.4 | 0.01 | 0.007 |
| *Sub-band 2–0 for substate $^2\Pi_{3/2}$* | | | | | | | | | |
| 1.5 | | | | 372353.0 | 0.54 | 0.486 | 373195.0 | 0.29 | 0.326 |
| 2.5 | 371493.0 | 0.30 | 0.305 | 372335.0 | 0.32 | 0.300 | 373513.7 | 0.52 | 0.558 |
| 3.5 | 371131.0 | 0.48 | 0.509 | 372309.7 | 0.23 | 0.210 | 373825.1 | 0.74 | 0.738 |
| 4.5 | 370761.9 | 0.66 | 0.656 | 372277.2 | 0.15 | 0.155 | 374129.1 | 1.02 | 0.872 |
| 5.5 | 370385.7 | 0.81 | 0.755 | 372237.6 | 0.12 | 0.117 | 374425.8 | 0.93 | 0.962 |
| 6.5 | 370002.4 | 0.86 | 0.813 | 372190.7 | 0.10 | 0.090 | 374715.2 | 1.02 | 1.011 |
| 7.5 | 369612.1 | 0.94 | 0.833 | 372136.6 | 0.08 | 0.070 | 374997.2 | 1.01 | 1.022 |
| 8.5 | 369214.8 | 0.89 | 0.821 | 372075.3 | 0.06 | 0.054 | 375271.8 | 0.90 | 0.999 |
| 9.5 | 368810.5 | 0.81 | 0.782 | | | | 375538.9 | 0.95 | 0.948 |
| 10.5 | 368399.2 | 0.79 | 0.724 | | | | 375798.7 | 0.89 | 0.876 |
| 11.5 | 367980.9 | 0.71 | 0.652 | | | | 376051.0 | 0.79 | 0.789 |
| 12.5 | 367555.8 | 0.61 | 0.573 | | | | 376295.9 | 0.73 | 0.695 |
| 13.5 | 367123.7 | 0.54 | 0.492 | | | | 376533.3 | 0.59 | 0.598 |
| 14.5 | 366684.8 | 0.47 | 0.413 | | | | 376763.2 | 0.50 | 0.504 |
| 15.5 | 366239.1 | 0.39 | 0.339 | | | | 376985.7 | 0.54 | 0.416 |
| 16.5 | 365786.5 | 0.32 | 0.273 | | | | 377200.7 | 0.34 | 0.336 |
| 17.5 | 365327.1 | 0.25 | 0.215 | | | | 377408.2 | 0.27 | 0.266 |

(*continued on next page*)

Table 1 (*continued*)

| $J$ | P($J$) | $S_{l,\mathrm{ob}}$ | $S_{l,\mathrm{cal}}$ | Q($J$) | $S_{l,\mathrm{ob}}$ | $S_{l,\mathrm{cal}}$ | R($J$) | $S_{l,\mathrm{ob}}$ | $S_{l,\mathrm{cal}}$ |
|---|---|---|---|---|---|---|---|---|---|
| 18.5 | 364860.9 | 0.17 | 0.166 | | | | 377608.1 | 0.21 | 0.207 |
| 19.5 | 364387.9 | 0.14 | 0.126 | | | | 377800.6 | 0.18 | 0.168 |
| 20.5 | 363908.2 | 0.11 | 0.094 | | | | 377985.5 | 0.13 | 0.118 |
| 21.5 | 363421.7 | 0.09 | 0.068 | | | | 378163.0 | 0.09 | 0.087 |
| 22.5 | 362928.5 | 0.07 | 0.049 | | | | 378332.8 | 0.07 | 0.062 |
| 23.5 | 362428.7 | 0.04 | 0.034 | | | | 378495.2 | 0.05 | 0.044 |
| 24.5 | 361922.1 | 0.03 | 0.024 | | | | 378649.9 | 0.03 | 0.031 |
| 25.5 | 361408.8 | 0.02 | 0.016 | | | | 378797.2 | 0.02 | 0.021 |
| 26.5 | 360888.8 | 0.02 | 0.011 | | | | 378936.8 | 0.02 | 0.014 |
| 27.5 | 360362.3 | 0.01 | 0.007 | | | | 379068.9 | 0.01 | 0.009 |
| 28.5 | | | | | | | 379193.4 | 0.01 | 0.006 |

for the latter measurements, problems with adsorption of NO or measurement of pressures are negligible.

By fitting all data for each band, including both sub-bands for each electronic substate, according to formulae (1) and (2), we derived values of squares of pure vibrational matrix elements and Herman-Wallis coefficient $C_0^{v'}$; for no band is a value of second coefficient $D_0^{v'}$ evaluated statistically significantly. Table 6 presents for each band a summary of results for pure vibrational matrix element and its statistical uncertainty, a band strength $S_b$ derived therefrom at 298 K, $C_0^{v'}$, and corresponding theoretical quantities to be explained separately. To convert those values of pure vibrational matrix element into coefficient $p_j$ in formula (6) through the following relation:

$$\langle v'|p(x)|0\rangle = \sum_{j=0}^{6} p_j \langle v'|x^j|0\rangle \tag{7}$$

we require further experimental information of two types: an accurate magnitude of $\langle 0|p(x)|0\rangle$ is obtained from application of the Stark effect on a molecular beam of $^{14}N^{16}O$ [16], which we associate with a polarity $^{-}NO^{+}$ and consequently a positive sign for $p_0$ as a sign convention, consistent with previous usage for CO [17]; as a value of $\langle 1|p(x)|0\rangle$ we accepted the more recent value of Spencer et al. [5]: both these data are reported in Table 6. Vibrational matrix elements of reduced displacement $x$ to various powers require for their evaluation a knowledge of coefficients $c_j$ of $z \equiv 2(R - R_e)/(R - R_e)$ in a function for potential energy,

$$V(z) = hcc_0 z^2 \left(1 + \sum_{j=1} c_j z^j\right) \tag{8}$$

and $\gamma \equiv 2B_e/\omega_e$ in terms of conventional spectral parameters. For this purpose we fitted values of vibrational terms $G(v)$ and rotational parameters $B_v$ listed by Amiot [14] to polynomials in $(v + l/2)$ up to $v = 22$; from the resulting coefficients $Y_{k,0}$ and $Y_{k,1}$, respectively, we applied expressions [18,19] of these quantities in terms of coefficients $c_j$ to derive directly the required values, involving no fitting. The results are $\gamma = 0.001790727$ and this formula for adiabatic potential energy,

$$\begin{aligned} V(z)/hc\ \mathrm{m}^{-1} = 53166650.6z^2(1 &- 1.91599565z \\ &+ 1.4963702z^2 - 0.3822858z^3 \\ &- 0.5913666z^4 - 1.6270814z^5 \\ &+ 25.86692z^6 - 95.37679z^7) \end{aligned} \tag{9}$$

with equilibrium internuclear distance $R_e = 1.1507825 \times 10^{-10}$ m of $^{14}N^{16}O$; for vibrational terms within the range of states, $v \leqslant 6$, for which we measured intensities, this formula is essentially exact, in that uncertainties of measured intensities dominate the eventual values of parameters for dipolar moment, but this formula might become unreliable for vibration-rotational terms at large values of $v$ and $J$. Using efficient procedures [12,19] to generate algebraic expressions for accurate vibrational matrix elements $\langle v'|p(x)|0\rangle$, we evaluated these quantities and solved seven simultaneous linear equations implied in formula (7) to evaluate seven coefficients $p_j$, according to the following formula:

Table 2
Values of quantum number $J''$ for total angular momentum of the lower state of a vibration-rotational transition in band 3–0, wave number/$m^{-1}$ of each apparent line in branches P, Q and R, and line strength $S_l/10^{-25}$ m observed and calculated for $^{14}N^{16}O$ in substates of electronic ground state $X^2\Pi_r$ at 296.6 K

| $J$ | P($J$) | $S_{l,ob}$ | $S_{l,cal}$ | Q($J$) | $S_{l,ob}$ | $S_{l,cal}$ | R($J$) | $S_{l,ob}$ | $S_{l,cal}$ |
|---|---|---|---|---|---|---|---|---|---|
| *Sub-band 3–0 for substate $^2\Pi_{1/2}$* | | | | | | | | | |
| 0.5 | | | | 554402.1 | 0.58 | 0.513 | 554888.3 | 1.09 | 1.048 |
| 1.5 | 553900.5 | 1.12 | 0.984 | 554386.7 | 0.09 | 0.200 | 555196.9 | 1.95 | 1.868 |
| 2.5 | 553550.7 | 1.71 | 1.681 | | | | 555495.3 | 2.47 | 2.598 |
| 3.5 | 553190.6 | 2.38 | 2.241 | | | | 555783.4 | 3.37 | 3.227 |
| 4.5 | 552820.2 | 2.81 | 2.669 | | | | 556061.1 | 3.76 | 3.733 |
| 5.5 | 552439.4 | 3.13 | 2.960 | | | | 556328.5 | 4.05 | 4.101 |
| 6.5 | 552048.4 | 3.21 | 3.118 | | | | 556585.6 | 4.04 | 4.324 |
| 7.5 | 551647.1 | 3.40 | 3.152 | | | | 556832.4 | 4.33 | 4.404 |
| 8.5 | 551235.5 | 3.33 | 3.078 | | | | 557068.8 | 4.36 | 4.350 |
| 9.5 | 550813.6 | 3.14 | 2.915 | | | | 557294.8 | 4.13 | 4.180 |
| 10.5 | 550381.4 | 2.82 | 2.686 | | | | 557510.5 | 3.59 | 3.916 |
| 11.5 | 549938.8 | 2.60 | 2.413 | | | | 557715.7 | 3.16 | 3.581 |
| 12.5 | 549486.0 | 2.43 | 2.116 | | | | 557910.5 | 2.83 | 3.202 |
| 13.5 | 549022.8 | 2.01 | 1.815 | | | | 558094.8 | 2.48 | 2.801 |
| 14.5 | 548549.3 | 1.73 | 1.522 | | | | 558268.6 | 2.01 | 2.399 |
| 15.5 | 548065.4 | 1.36 | 1.250 | | | | 558432.0 | 1.59 | 1.803 |
| 16.5 | 547571.2 | 1.26 | 1.006 | | | | 558584.8 | 1.51 | 1.656 |
| 17.5 | 547066.8 | 0.90 | 0.794 | | | | 558727.1 | 1.38 | 1.336 |
| 18.5 | 546551.9 | 0.89 | 0.614 | | | | 558858.9 | 0.99 | 1.057 |
| 19.5 | 546026.8 | 0.58 | 0.466 | | | | 558980.0 | 0.80 | 0.821 |
| 20.5 | 545491.3 | 0.43 | 0.347 | | | | 559090.5 | 0.57 | 0.626 |
| 21.5 | 544945.6 | 0.17 | 0.254 | | | | 559190.3 | 0.31 | 0.468 |
| 22.5 | 544389.5 | 0.09 | 0.182 | | | | 559279.5 | 0.23 | 0.344 |
| 23.5 | | | | | | | 559358.0 | 0.16 | 0.248 |
| *Sub-band 3–0 for substate $^2\Pi_{3/2}$* | | | | | | | | | |
| 1.5 | | | | 554320.0 | 0.88 | 1.008 | 555153.0 | 0.62 | 0.696 |
| 2.5 | 553459.9 | 0.49 | 0.622 | 554292.9 | 0.47 | 0.622 | 555459.0 | 1.10 | 1.209 |
| 3.5 | 553088.9 | 1.08 | 1.033 | 554255.0 | 0.31 | 0.434 | 555754.1 | 1.53 | 1.619 |
| 4.5 | 552707.2 | 1.46 | 1.323 | 554206.3 | 0.41 | 0.320 | 556038.3 | 1.98 | 1.938 |
| 5.5 | 552314.7 | 1.80 | 1.514 | 554146.7 | 0.36 | 0.243 | 556311.5 | 2.14 | 2.187 |
| 6.5 | 551911.5 | 1.78 | 1.619 | 554076.3 | 0.26 | 0.186 | 556573.7 | 2.31 | 2.307 |
| 7.5 | 551497.7 | 1.69 | 1.647 | 553995.1 | 0.15 | 0.144 | 556825.0 | 2.26 | 2.361 |
| 8.5 | 551073.3 | 1.82 | 1.612 | | | | 557065.3 | 1.82 | 2.336 |
| 9.5 | 550638.3 | 1.58 | 1.525 | | | | 557294.5 | 2.06 | 2.245 |
| 10.5 | 550192.7 | 1.36 | 1.401 | | | | 557512.7 | 1.91 | 2.099 |
| 11.5 | 549736.5 | 1.27 | 1.253 | | | | 557719.9 | 1.81 | 1.905 |
| 12.5 | 549269.8 | 1.02 | 1.093 | | | | 557916.1 | 1.67 | 1.706 |
| 13.5 | 548792.7 | 1.04 | 0.931 | | | | 558101.2 | 1.26 | 1.485 |
| 14.5 | 548305.1 | 0.76 | 0.775 | | | | 558275.3 | 1.27 | 1.266 |
| 15.5 | 547807.0 | 0.42 | 0.632 | | | | 558438.3 | 1.00 | 1.056 |
| 16.5 | 547298.5 | 0.62 | 0.504 | | | | 558590.2 | 0.94 | 0.864 |
| 17.5 | 546779.6 | 0.45 | 0.394 | | | | 558731.0 | 0.51 | 0.692 |
| 18.5 | 546250.4 | 0.26 | 0.302 | | | | 558860.8 | 0.50 | 0.544 |
| 19.5 | 545710.8 | 0.35 | 0.227 | | | | 558979.5 | 0.40 | 0.419 |
| 20.5 | 545160.9 | 0.11 | 0.167 | | | | 559087.0 | 0.23 | 0.317 |
| 21.5 | 544600.6 | 0.05 | 0.121 | | | | 559183.5 | 0.35 | 0.235 |
| 22.5 | | | | | | | 559268.9 | 0.08 | 0.172 |
| 23.5 | | | | | | | 559343.2 | 0.06 | 0.123 |

Table 3
Values of quantum number $J''$ for total angular momentum of the lower state of a vibration-rotational transition in band 4–0, wave number/$m^{-1}$ of each apparent line in branches P, Q and R, and line strength $S_l/10^{-26}$ m observed and calculated for $^{14}N^{16}O$ in substates of electronic ground state $X^2\Pi_r$ at 298.8 K

| $J$ | P($J$) | $S_{l,ob}$ | $S_{l,cal}$ | Q($J$) | $S_{l,ob}$ | $S_{l,cal}$ | R($J$) | $S_{l,ob}$ | $S_{l,cal}$ |
|---|---|---|---|---|---|---|---|---|---|
| *Sub-band 4–0 for substate $^2\Pi_{1/2}$* | | | | | | | | | |
| 0.5 | | | | 733598.3 | 0.16 | 0.232 | 734079.3 | 0.36 | 0.472 |
| 1.5 | 733096.7 | 0.49 | 0.445 | 733577.7 | 0.10 | 0.091 | 734379.3 | 0.92 | 0.839 |
| 2.5 | 732741.7 | 0.75 | 0.760 | 733543.3 | 0.03 | 0.056 | 734665.6 | 1.14 | 1.164 |
| 3.5 | 732373.0 | 1.03 | 1.015 | | | | 734938.2 | 1.40 | 1.442 |
| 4.5 | 731990.5 | 1.31 | 1.210 | | | | 735197.0 | 1.56 | 1.665 |
| 5.5 | 731594.3 | 1.47 | 1.343 | | | | 735442.0 | 1.74 | 1.825 |
| 6.5 | 731184.3 | 1.48 | 1.415 | | | | 735673.2 | 1.73 | 1.920 |
| 7.5 | 730760.6 | 1.55 | 1.432 | | | | 735890.7 | 1.70 | 1.952 |
| 8.5 | 730323.1 | 1.51 | 1.400 | | | | 736094.3 | 1.59 | 1.925 |
| 9.5 | 729871.9 | 1.44 | 1.327 | | | | 736284.0 | 1.53 | 1.846 |
| 10.5 | 729406.8 | 1.49 | 1.224 | | | | 736459.9 | 1.46 | 1.727 |
| 11.5 | 728928.0 | 1.21 | 1.101 | | | | 736622.0 | 1.31 | 1.577 |
| 12.5 | 728435.5 | 1.00 | 0.967 | | | | 736770.1 | 1.26 | 1.408 |
| 13.5 | 727929.1 | 0.90 | 0.830 | | | | 736904.3 | 1.06 | 1.230 |
| 14.5 | 727408.9 | 0.76 | 0.697 | | | | 737024.5 | 0.89 | 1.052 |
| 15.5 | 726874.9 | 0.64 | 0.573 | | | | 737130.7 | 0.74 | 0.882 |
| 16.5 | 726327.1 | 0.51 | 0.462 | | | | 737223.0 | 0.56 | 0.725 |
| 17.5 | 725765.5 | 0.38 | 0.365 | | | | 737301.2 | 0.58 | 0.584 |
| 18.5 | 725190.1 | 0.33 | 0.283 | | | | 737365.3 | 0.25 | 0.462 |
| 19.5 | 724600.8 | 0.24 | 0.215 | | | | 737415.3 | 0.29 | 0.358 |
| 20.5 | 723997.8 | 0.20 | 0.160 | | | | 737451.2 | 0.27 | 0.273 |
| 21.5 | 723380.9 | 0.14 | 0.118 | | | | 737472.9 | 0.24 | 0.200 |
| 22.5 | 722750.2 | 0.09 | 0.085 | | | | 737480.5 | 0.03 | 0.150 |
| 23.5 | 722105.6 | 0.08 | 0.060 | | | | 737473.8 | 0.08 | 0.108 |
| 24.5 | 721447.3 | 0.02 | 0.041 | | | | 737452.9 | 0.11 | 0.077 |
| 25.5 | 720775.1 | 0.04 | 0.028 | | | | | | |
| 26.5 | 720089.1 | 0.02 | 0.019 | | | | | | |
| *Sub-band 4–0 for substate $^2\Pi_{3/2}$* | | | | | | | | | |
| 1.5 | | | | 733486.5 | 0.48 | 0.458 | 734310.4 | 0.34 | 0.317 |
| 2.5 | 732626.4 | 0.23 | 0.284 | 733450.3 | 0.35 | 0.282 | 734603.7 | 0.55 | 0.554 |
| 3.5 | 732246.3 | 0.33 | 0.474 | 733399.7 | 0.18 | 0.197 | 734882.5 | 0.79 | 0.750 |
| 4.5 | 731851.9 | 0.54 | 0.608 | 733334.7 | 0.15 | 0.146 | 735146.8 | 0.92 | 0.909 |
| 5.5 | 731443.1 | 0.54 | 0.698 | 733255.2 | 0.12 | 0.110 | 735396.5 | 1.06 | 1.032 |
| 6.5 | 731020.1 | 0.64 | 0.749 | 733161.3 | 0.13 | 0.085 | 735631.6 | 1.23 | 1.119 |
| 7.5 | 730582.7 | 0.69 | 0.765 | 733053.0 | 0.09 | 0.065 | 735852.1 | 1.22 | 1.169 |
| 8.5 | 730131.1 | 0.70 | 0.751 | | | | 736058.0 | 1.11 | 1.184 |
| 9.5 | 729665.3 | 0.66 | 0.713 | | | | 736249.2 | 1.17 | 1.167 |
| 10.5 | 729185.4 | 0.63 | 0.657 | | | | 736425.9 | 1.07 | 1.122 |
| 11.5 | 728691.2 | 0.59 | 0.590 | | | | 736587.9 | 1.06 | 1.055 |
| 12.5 | 728183.0 | 0.53 | 0.516 | | | | 736735.2 | 0.82 | 0.970 |
| 13.5 | 727660.6 | 0.44 | 0.441 | | | | 736868.0 | 0.65 | 0.873 |
| 14.5 | 727124.2 | 0.38 | 0.369 | | | | 736986.0 | 0.53 | 0.771 |
| 15.5 | 726573.7 | 0.30 | 0.302 | | | | 737089.4 | 0.39 | 0.667 |
| 16.5 | 726009.3 | 0.25 | 0.242 | | | | 737178.2 | 0.21 | 0.566 |
| 17.5 | 725430.8 | 0.24 | 0.190 | | | | 737252.3 | 0.18 | 0.472 |
| 18.5 | 724838.4 | 0.18 | 0.146 | | | | 737311.7 | 0.13 | 0.386 |
| 19.5 | 724232.0 | 0.15 | 0.110 | | | | 737356.4 | 0.16 | 0.310 |
| 20.5 | 723611.7 | 0.09 | 0.089 | | | | 737386.5 | 0.11 | 0.245 |

Table 3 (*continued*)

| $J$ | P($J$) | $S_{J,\mathrm{ob}}$ | $S_{J,\mathrm{cal}}$ | Q($J$) | $S_{J,\mathrm{ob}}$ | $S_{J,\mathrm{cal}}$ | R($J$) | $S_{J,\mathrm{ob}}$ | $S_{J,\mathrm{cal}}$ |
|---|---|---|---|---|---|---|---|---|---|
| 21.5 | 722977.5 | 0.07 | 0.059 | | | | 737401.8 | 0.10 | 0.190 |
| 22.5 | 722329.5 | 0.04 | 0.042 | | | | 737402.5 | 0.08 | 0.145 |
| 23.5 | 721667.5 | 0.04 | 0.030 | | | | 737388.5 | 0.05 | 0.108 |
| 24.5 | 720991.8 | 0.01 | 0.020 | | | | 737359.8 | 0.05 | 0.080 |

$$p(x)/10^{-30}\ \mathrm{C\,m} = 0.558274 - 8.649479x + 5.048787x^2 - 0.866241x^3 + 28.3255x^4 - 81.2569x^5 + 270.714x^6 \qquad (10)$$

As presented in Table 6, the signs of $\langle v'|p(x)|0\rangle$ are selected to produce best agreement between experimental values of Herman-Wallis coefficient $C_0^{v'}$ and values calculated on the basis of formula (10); these calculated values of $C_0^{v'}$ and also $D_0^{v'}$ are included in Table 6. With points resulting from calculations of molecular electronic structure [20] for comparison, formula (10) is plotted in Fig. 2; the range/$10^{-10}$ m of validity of this formula, corresponding to the amplitude of vibration in state $v = 6$, is [1.0, 1.38]. With these values of $\langle v'p(x)|0\rangle$, $C_0^{v'}$, $D_0^{v'}$ for each band and the wave number of each spectral feature, as reported in Tables 1–5, we calculated with formula (1) the strength of each feature for comparison with observed strengths, also presented in Tables 1–5.

## 5. Discussion

With only seven parameters in a radial function for electric dipolar moment—coefficients of $x$ to various powers in formula (10)—and with $\gamma$ and seven parameters $c_j$, $j > 0$, in a radial function for potential energy in formula (9), we reproduce the strengths of more than 500 spectral features, each having two components of supposed equal contribution, in our measurements of bands 2–0 up to 6–0, almost within the uncertainties of their measurement. With the same parameters we can likewise reproduce more than 100 separate measurements on band 1–0 [5] and another 79 measurements on bands 3–1 [9] and 2–1 [8]; the latter results are more compatible with the results [5] on band 1–0 that we used than with earlier measurements [4]. Measurements of strengths of lines in some R branches are complicated by overlapping of features due to not only the presence of band heads but also branches of separate substates. Except for band 2–0, our experimental magnitudes of Herman-Wallis coefficient $C_0^{v'}$ are consistent with calculated values; as integrated areas of lines are small and subject to uncertainties from interferences between overlapping lines, evaluation of a quadratic term to evaluate $D_0^{v'}$ is impracticable in this work. Both reported values $C_0^2 = (3.57 \pm 0.14) \times 10^{-3}$ [6] and $(3.66 \pm 0.08) \times 10^{-3}$ [7] are consistent with our calculated value $3.75 \times 10^3$ indicated in Table 6, but a reported value $D_0^2 = (4.74 \pm 0.50) \times 10^{-5}$ [7] differs appreciably from our calculated value $1.64 \times 10^{-5}$; even with great spectral resolution and full separation of Λ doublets, an accurate evaluation of coefficient $D_0^{v'}$ is evidently difficult. Because the total strength of each band, estimated as the sum of measured strengths according to formula (3), is consistent with the band strength, presented in Table 6, that is derived from the deduced pure vibrational matrix element based on strengths of individual features through formula (4), likely the calculated strengths of features, which are double the strengths of each component of a feature, are more reliable than the observed strengths. The ratios of strengths of successive vibration-rotational bands—65.2, 48.1, 22.1, 13.4, 8.6—of NO decrease regularly with increasing vibrational quantum number $v$, whereas the corresponding ratios—128, 177, 289, ~250—for CO tend to increase in the same order [20]; the radial functions for electric dipolar moment of NO and CO share common features of two extrema, as exhibited in Fig. 2, with a consequent reversal of polarity between these two extrema and small magnitudes of permanent electric moment $p(R_e)$. In each case the polarities, $^-NO^+$ and $^-CO^+$, at that condition

Table 4
Values of quantum number $J''$ for total angular momentum of the lower state of a vibration-rotational transition in band 5–0, wave number/$m^{-1}$ of each apparent line in branches P, Q and R, and line strength $S_l/10^{-28}$ m observed and calculated for $^{14}N^{16}O$ in substates of electronic ground state $X^2\Pi_r$ at 297.2 K

| $J$ | P($J$) | $S_{l,ob}$ | $S_{l,cal}$ | Q($J$) | $S_{l,ob}$ | $S_{l,cal}$ | R($J$) | $S_{l,ob}$ | $S_{l,cal}$ |
|---|---|---|---|---|---|---|---|---|---|
| *Sub-band 5–0 for substate $^2\Pi_{1/2}$* | | | | | | | | | |
| 0.5 | | | | 909998.7 | 1.67 | 1.748 | 910474.5 | 3.50 | 3.523 |
| 1.5 | 909497.1 | 3.43 | 3.385 | 909972.9 | 0.71 | 0.682 | 910765.9 | 6.16 | 6.220 |
| 2.5 | 909136.9 | 6.56 | 5.820 | 909929.9 | 0.42 | 0.421 | 911040.1 | 8.26 | 8.575 |
| 3.5 | 908759.6 | 7.99 | 7.851 | 909869.8 | 0.10 | 0.295 | 911297.2 | 10.7 | 10.56 |
| 4.5 | 908365.0 | 9.41 | 9.367 | | | | 911536.9 | 12.7 | 12.10 |
| 5.5 | 907953.2 | 10.3 | 10.46 | | | | 911759.5 | 13.9 | 13.18 |
| 6.5 | 907524.3 | 11.6 | 10.09 | | | | 911964.8 | 12.7 | 13.77 |
| 7.5 | 907078.1 | 11.2 | 11.28 | | | | 912152.8 | 14.1 | 13.90 |
| 8.5 | 906614.7 | 10.4 | 11.09 | | | | 912323.5 | 14.5 | 13.61 |
| 9.5 | 906134.0 | 10.4 | 10.57 | | | | 912477.0 | 12.6 | 12.96 |
| 10.5 | 905636.1 | 9.68 | 9.807 | | | | 912613.0 | 13.2 | 12.04 |
| 11.5 | 905121.0 | 8.55 | 8.866 | | | | 912731.8 | 11.7 | 10.91 |
| 12.5 | 904588.6 | 7.43 | 7.826 | | | | 912833.1 | 7.72 | 9.668 |
| 13.5 | 904038.9 | 6.67 | 6.752 | | | | 912917.0 | 8.33 | 8.383 |
| 14.5 | 903471.9 | 5.89 | 5.701 | | | | 912983.4 | 6.30 | 7.117 |
| 15.5 | 902887.6 | 4.77 | 4.712 | | | | 913032.4 | 4.48 | 5.920 |
| 16.5 | 902286.1 | 4.01 | 3.816 | | | | 913063.9 | 4.01 | 4.827 |
| 17.5 | 901667.2 | 2.56 | 3.030 | | | | 913077.8 | 3.29 | 3.860 |
| 18.5 | 901031.0 | 2.37 | 2.359 | | | | 913074.2 | 3.25 | 3.028 |
| 19.5 | 900377.5 | 1.84 | 1.801 | | | | 913052.9 | 2.98 | 2.331 |
| 20.5 | 899706.6 | 1.40 | 1.350 | | | | 913014.0 | 0.79 | 1.762 |
| 21.5 | 899018.5 | 1.18 | 0.993 | | | | 912957.4 | 1.58 | 1.307 |
| 22.5 | 898313.0 | 0.45 | 0.707 | | | | 912883.1 | 0.82 | 0.952 |
| 23.5 | 897590.1 | 0.46 | 0.509 | | | | 912791.1 | 0.97 | 0.681 |
| 24.5 | | | | | | | 912681.3 | 0.44 | 0.479 |
| *Sub-band 5–0 for substate $^2\Pi_{3/2}$* | | | | | | | | | |
| 1.5 | | | | 909855.9 | 3.10 | 3.438 | 910670.7 | 2.60 | 2.321 |
| 2.5 | 908995.8 | 1.93 | 2.170 | 909810.7 | 2.31 | 2.120 | 910951.4 | 3.49 | 3.996 |
| 3.5 | 908606.7 | 3.86 | 3.635 | 909747.4 | 1.28 | 1.481 | 911213.8 | 6.15 | 5.303 |
| 4.5 | 908199.5 | 4.33 | 4.696 | 909666.0 | 0.90 | 1.093 | 911458.1 | 6.32 | 6.292 |
| 5.5 | 907774.4 | 4.79 | 5.423 | 909566.6 | 0.99 | 0.829 | 911684.2 | 7.85 | 6.974 |
| 6.5 | 907331.4 | 5.73 | 5.850 | 909449.1 | 0.63 | 0.636 | 911892.1 | 6.32 | 7.357 |
| 7.5 | 906870.5 | 7.16 | 6.007 | 909313.5 | 0.48 | 0.491 | 912081.8 | 7.80 | 7.461 |
| 8.5 | 906391.7 | 7.06 | 5.930 | | | | 912253.2 | 8.79 | 7.319 |
| 9.5 | 905895.1 | 6.15 | 5.661 | | | | 912406.4 | 7.05 | 6.970 |
| 10.5 | 905380.6 | 5.44 | 5.247 | | | | 912541.4 | 7.11 | 6.461 |
| 11.5 | 904848.4 | 4.64 | 4.735 | | | | 912658.1 | 6.36 | 5.841 |
| 12.5 | 904298.5 | 4.59 | 4.166 | | | | 912756.6 | 5.89 | 5.157 |
| 13.5 | 903730.8 | 3.36 | 3.580 | | | | 912836.8 | 6.35 | 4.452 |
| 14.5 | 903145.5 | 2.87 | 3.008 | | | | 912898.7 | 3.98 | 3.761 |
| 15.5 | 902542.6 | 2.44 | 2.473 | | | | 912942.4 | 3.04 | 3.111 |
| 16.5 | 901922.0 | 2.37 | 1.991 | | | | 912967.9 | 2.16 | 2.521 |
| 17.5 | 901283.8 | 1.90 | 1.570 | | | | 912975.0 | 1.64 | 2.003 |
| 18.5 | 900628.1 | 1.33 | 1.214 | | | | 912963.9 | 1.08 | 1.560 |
| 19.5 | 899954.8 | 0.91 | 0.921 | | | | 912934.6 | 0.85 | 1.192 |
| 20.5 | 899264.0 | 0.77 | 0.685 | | | | 912886.9 | 1.15 | 0.894 |
| 21.5 | 898555.7 | 0.47 | 0.500 | | | | 912821.0 | 0.64 | 0.658 |

Table 5
Values of quantum number $J''$ for total angular momentum of the lower state of a vibration-rotational transition in band 6–0, wave number/$m^{-1}$ of each apparent line in branches P, Q and R, and line strength $S_l/10^{-28}$ m observed and calculated for $^{14}N^{16}O$ in substates of electronic ground state $X^2\Pi_r$ at 297.4 K

| $J$ | P($J$) | $S_{l,ob}$ | $S_{l,cal}$ | Q($J$) | $S_{l,ob}$ | $S_{l,cal}$ | R($J$) | $S_{l,ob}$ | $S_{l,cal}$ |
|---|---|---|---|---|---|---|---|---|---|
| *Sub-band 6–0 for substate $^2\Pi_{1/2}$* | | | | | | | | | |
| 0.5 | | | | 1083605.8 | 0.22 | 0.202 | 1084076.4 | 0.44 | 0.406 |
| 1.5 | 1083104.2 | 0.47 | 0.392 | 1083574.8 | 0.12 | 0.079 | 1084359.1 | 0.79 | 0.717 |
| 2.5 | 1082738.8 | 0.68 | 0.674 | 1083523.1 | 0.04 | 0.049 | 1084621.2 | 1.17 | 0.988 |
| 3.5 | 1082352.8 | 0.96 | 0.906 | | | | 1084862.6 | 1.38 | 1.214 |
| 4.5 | 1081946.1 | 1.15 | 1.087 | | | | 1085083.3 | 1.38 | 1.391 |
| 5.5 | 1081518.7 | 1.14 | 1.215 | | | | 1085283.4 | 1.52 | 1.513 |
| 6.5 | 1081070.7 | 1.27 | 1.290 | | | | 1085462.6 | 1.53 | 1.580 |
| 7.5 | 1080602.0 | 1.24 | 1.314 | | | | 1085621.2 | 1.55 | 1.593 |
| 8.5 | 1080112.5 | 1.35 | 1.293 | | | | 1085758.9 | 1.53 | 1.558 |
| 9.5 | 1079602.4 | 1.29 | 1.234 | | | | 1085875.9 | 1.47 | 1.483 |
| 10.5 | 1079071.5 | 1.04 | 1.145 | | | | 1085972.1 | 1.32 | 1.375 |
| 11.5 | 1078519.9 | 1.08 | 1.037 | | | | 1086047.4 | 1.29 | 1.246 |
| 12.5 | 1077947.6 | 0.94 | 0.916 | | | | 1086101.8 | 1.16 | 1.103 |
| 13.5 | 1077354.5 | 0.64 | 0.791 | | | | 1086135.3 | 1.30 | 0.955 |
| 14.5 | 1076740.6 | 0.79 | 0.669 | | | | 1086147.8 | 0.65 | 0.810 |
| 15.5 | 1076105.9 | 0.60 | 0.553 | | | | 1086139.3 | 0.51 | 0.673 |
| 16.5 | 1075450.4 | 0.54 | 0.449 | | | | 1086109.9 | 0.77 | 0.549 |
| 17.5 | 1074774.1 | 0.30 | 0.357 | | | | 1086059.4 | 0.37 | 0.438 |
| 18.5 | 1074077.0 | 0.22 | 0.278 | | | | 1085987.8 | 0.33 | 0.343 |
| 19.5 | 1073359.0 | 0.24 | 0.212 | | | | 1085895.0 | 0.28 | 0.264 |
| 20.5 | | | | | | | 1085781.1 | 0.18 | 0.199 |
| *Sub-band 6–0 for substate $^2\Pi_{3/2}$* | | | | | | | | | |
| 1.5 | | | | 1083430.4 | 0.34 | 0.397 | 1084236.2 | 0.25 | 0.268 |
| 2.5 | 1082570.4 | 0.28 | 0.251 | 1083376.1 | 0.24 | 0.245 | 1084504.1 | 0.50 | 0.460 |
| 3.5 | 1082172.1 | 0.47 | 0.421 | 1083300.1 | 0.15 | 0.171 | 1084750.2 | 0.68 | 0.610 |
| 4.5 | 1081752.3 | 0.41 | 0.545 | 1083202.3 | 0.15 | 0.126 | 1084974.5 | 0.73 | 0.723 |
| 5.5 | 1081310.8 | 0.66 | 0.630 | | | | 1085176.9 | 0.68 | 0.801 |
| 6.5 | 1080847.7 | 0.74 | 0.680 | | | | 1085357.5 | 0.72 | 0.844 |
| 7.5 | 1080363.2 | 0.79 | 0.699 | | | | 1085516.3 | 0.69 | 0.855 |
| 8.5 | 1079857.1 | 0.66 | 0.691 | | 1085653.2 | 0.93 | 0.838 | | |
| 9.5 | 1079329.6 | 0.59 | 0.660 | | 1085768.3 | 0.86 | 0.797 | | |
| 10.5 | 1078780.6 | 0.64 | 0.613 | | 1085861.4 | 0.68 | 0.738 | | |
| 11.5 | 1078210.3 | 0.65 | 0.553 | | 1085932.8 | 0.66 | 0.667 | | |
| 12.5 | 1077618.5 | 0.41 | 0.488 | | 1085982.2 | 0.49 | 0.588 | | |
| 13.5 | 1077005.5 | 0.35 | 0.419 | | 1086009.8 | 0.52 | 0.507 | | |
| 14.5 | 1076371.2 | 0.38 | 0.353 | | 1086015.5 | 0.45 | 0.428 | | |
| 15.5 | 1075715.6 | 0.25 | 0.290 | | 1085999.3 | 0.43 | 0.354 | | |
| 16.5 | 1075038.7 | 0.23 | 0.234 | | 1085961.3 | 0.29 | 0.286 | | |
| 17.5 | 1074340.7 | 0.25 | 0.185 | | 1085901.4 | 0.28 | 0.227 | | |
| 18.5 | 1073621.5 | 0.14 | 0.143 | | 1085819.6 | 0.13 | 0.177 | | |
| 19.5 | | | | | 1085716.0 | 0.08 | 0.135 | | |

contradict expectations from crude consideration of conventional electronegativities.

For band 3–0 of $^{14}N^{16}O$ our strength $S_b = (1.48 \pm 0.01) \times 10^{-23}$ m, reported in Table 6, is consistent with the most recent result, $S_b = (1.52 \pm 0.08) \times 10^{-23}$ m, from measurements on samples with He or Ar at pressures large enough to obliterate rotational structure [21]. Like our independent reproduction of the strength of band 2–0 [7], this agreement confirms the efficacy of our procedure of measurement involving fitting, with a mixed gaussian and lorentzian profile, of

Table 6
Origins of vibration-rotational bands $v'$–0, experimental matrix elements of electric dipolar moment, band strengths at 298 K and experimental and calculated values of Herman-Wallis coefficients for $^{14}N^{16}O$

| $v'$ | $\tilde{\nu}_c/m^{-1}$ | $\langle v'\|p(x)\|0\rangle$/C m | $S_b/m$[a] | $C_0v'/\times10^{-3}$[b] | $C_0v'/\times10^{-3}$[c] | $D_0v'/\times10^{-5}$[c] |
|---|---|---|---|---|---|---|
| 0 | 0 | $(5.29433 \pm 0.00066)\times10^{-31}$[d] | – | – | 0 | −10.5 |
| 1 | 187598.9277 | $-(2.5778 \pm 0.0017)\times10^{-31}$[e] | $4.63\times10^{-20}$[e] | $0.51 \pm 0.13$[e] | 0.414 | 0.178 |
| 2 | 372388.7584 | $(2.2579 \pm 0.0035)\times10^{-32}$[f] | $7.10\times10^{-22}$ | $2.52 \pm 0.22$ | 3.751 | 1.638 |
| 3 | 554374.4427 | $-(2.6605 \pm 0.0077)\times10^{-33}$[f] | $1.48\times10^{-23}$ | $4.99 \pm 0.57$ | 5.675 | 1.606 |
| 4 | 733560.2566 | $(4.9386 \pm 0.0150)\times10^{-34}$[f] | $6.69\times10^{-25}$ | $5.86 \pm 0.48$ | 5.527 | 0.074 |
| 5 | 909949.6772 | $-(1.2135 \pm 0.0058)\times10^{-34}$[f] | $5.01\times10^{-26}$ | $3.44 \pm 0.73$ | 4.822 | −2.011 |
| 6 | 1083544.980 | $(3.791 \pm 0.019)\times10^{-35}$[f] | $5.83\times10^{-27}$ | $3.18 \pm 0.89$ | 3.892 | −1.917 |

[a] calculated from matrix element in preceding column
[b] fitted from spectra with formulae (1) and (2)
[c] calculated on the basis of formulae (9) and (10)
[d] $|\langle 0|p(x)|0\rangle|$ from Ref. [15]
[e] $|\langle 1|p(x)|0\rangle|$, $S_b$ and $C_0^1$ from Ref. [5]
[f] uncertainties from fits of line strengths; relative error of absolute magnitude is likely ±2%.

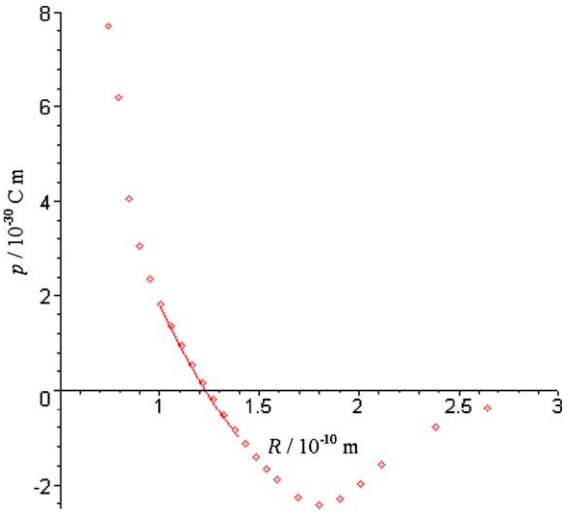


Fig. 2. Radial function $p(R)$ of $^{14}N^{16}O$ from spectral data (solid curve) with points from calculations of molecular electronic structure from reference 19 for comparison.

each perceived feature that comprises two lines in close proximity, each of which has hyperfine structure due to coupling of rotational and angular momenta and the nuclear quadrupolar moment of $^{14}N$. As already explained, our value of the strength of band 3–0 results from an accurate ratio with band 2–0. Our strength of band 2–0 is also consistent with a measurement of matrix element for band 3–1 [9], which implies a corresponding matrix element $(2.284 \pm 0.029)\times10^{-32}$ C m for band 2–0. For band 4–0, extensive quantitative measurements of intensity are unavailable. For bands 5–0 and 6–0 our results reported here supersede those reported in previous publications [10,11].

From calculations of molecular electronic structure [20] that indicate the polarity at $R_e$ to be $^{-}NO^{+}$ as we applied, points for electric dipolar moment of NO, included in Fig. 2, at internuclear distances in the range of experimental observations lie consistently slightly above a curve corresponding to formula (10). These differences reflect a systematic deficiency of those calculations, previously explained [20] to be related to an underestimate of the electron affinity of oxygen, with respect to the permanent dipolar moment, $p(R_e)$; as the latter value that is based essentially on an accurate measurement through the Stark effect [16] is included in the basis of our generation of formula (10), the differences persist between our experimentally derived function and the calculated points [20]. Apart from that slight systematic shift, our results are entirely compatible with those computational results. Some estimates [22] of band strengths from results of other, unpublished calculations of molecular electronic structure are greater than either reported value for band 2–0 [6,7] and thus also our present value, but smaller [22] for band 5–0 than our experimental result; comparison with graphical depictions [22] indicates that those estimates of line strengths in bands 3–0

and 4–0 are also only roughly consistent with our direct measurements. Further, accurate calculations are desirable.

## 6. Conclusion

Based on experimental measurements of line strengths in five bands of the infrared spectrum of $^{14}N^{16}O$ in vibration-rotational transitions within each substate of its electronic ground state X $^2\Pi_r$, we have derived a formula for electric dipolar moment as a function of internuclear distance that reproduces satisfactorily the observed strengths of about 700 features in vibration-rotational spectra up to $v = 6$. Our data will facilitate monitoring the concentration of NO in the terrestrial atmosphere.

## Acknowledgments

Taiwan's National Science Council (grant NSC92-2113-M007-034) and Ministry of Education Program for Promoting Academic Excellence of Universities (grant 89-FA04-AA) provided support for this project.

## References

[1] L.A. Pugh, K.N. Rao, Intensities from infrared spectra, in: K.N. Rao (Ed.), Molecular spectroscopy: modern research, Academic Press, New York, 1976, pp. 165–181.

[2] M.A.H. Smith, C.P. Rinsland, B. Fridovich, K.N. Rao, Intensities and collisional broadening parameters from infrared spectra, in: K.N. Rao (Ed.), Molecular Spectroscopy: Modern Research, Academic Press, New York, 1985, pp. 111–248.

[3] M.A.H. Smith, C.P. Rinsland, V.M. Devi, L.S. Rothman, K.N. Rao, Intensities and collisional-broadening parameters from infrared spectra—an update, in: K.N. Rao, A. Weber (Eds.), Spectroscopy of the Earth's Atmosphere and Interstellar Media, Academic Press, Boston, 1992, pp. 153–260.

[4] J. Ballard, W.B. Johnston, B.J. Kerridge, J.J. Remedies, Experimental spectral line parameters in the band $1 \leftarrow 0$ of NO, J. Mol. Spectrosc. 127 (1988) 70–82.

[5] M.N. Spencer, C. Chackerian, L.P. Giver, L.R. Brown, The fundamental band of NO: frequency and shape parameters for rovibrational lines, J. Mol. Spectrosc. 165 (1994) 506–524.

[6] A.S. Pine, A.G. Maki, N.-Y. Chou, Pressure broadening, line shapes and intensity measurements in the band $2 \leftarrow 0$ of NO, J. Mol. Spectrosc. 114 (1985) 132–147.

[7] J.-Y. Mandin, V. Dana, L. Regalia, A. Barbe, X. Thomas, Λ splittings and line intensities in the first overtone of NO, J. Mol. Spectrosc. 185 (1997) 347–355.

[8] V. Dana, J.-Y. Mandin, L.H. Coudert, M. Badaoui, F. LeRoy, G. Guelachvili, L.S. Rothman, Λ splittings and line intensities in the hot band $2 \leftarrow 1$ of NO, J. Mol. Spectrosc. 165 (1994) 525–540.

[9] J.Y. Mandin, V. Dana, L. Regalia, A. Barbe, P. von der Heyden, Λ splittings and line intensities in the hot band $3 \leftarrow 1$ of $^{14}N^{16}O$; the spectrum of nitric oxide in the first-overtone region, J. Mol. Spectrosc. 187 (1998) 200–205.

[10] Y.-P. Lee, J.F. Ogilvie, Strengths of absorption lines in vibration-rotational band $v = 5 \leftarrow v = 0$ of $^{14}N^{16}O$ $X^2\Pi_r$, Infrared Phys. 28 (1988) 321–324.

[11] Y.-P. Lee, S.-L. Cheah, J.F. Ogilvie, Strengths of absorption features in vibration-rotational band $v = 6 \leftarrow v = 0$ of $^{14}N^{I6}O$ $X^2\Pi_r$ in the near infrared region, Infrared Phys. Technol. 44 (2003) 199–205.

[12] J.F. Ogilvie, The Vibrational and Rotational Spectrometry of Diatomic Molecules, Academic Press, London, UK, 1998, and references therein.

[13] J.D. Ray, R.A. Ogg, A new method of preparing nitric oxide, J. Amer. Chem. Soc. 78 (1956) 5893.

[14] C. Meyer, C. Haeusler, Spectre de vibration-rotation de l'oxyde nitrique NO; etude de la bande $4 \leftarrow 0$ a 7336 $cm^{-1}$, C. R. Acad. Sci. Paris 280 (1965) 4182–4185.

[15] C. Amiot, The infrared emission spectrum of NO; analysis of the sequence $\Delta v = 3$ up to $v = 22$, J. Mol. Spectrosc. 94 (1982) 150–172.

[16] R.M. Neumann, Highly precise radio-frequency spectrum of $^{14}N^{16}O$, Astrophys. J. 161 (1970) 779–784.

[17] J.F. Ogilvie, S.-L. Cheah, Y.-P. Lee, S.P.A. Sauer, Infrared spectra of CO in absorption and evaluation of radial functions for potential energy and electric dipolar moment, Theor. Chem. Ace. 108 (2002) 85–97, and unpublished results.

[18] J.F. Ogilvie, Spectral energy coefficients for vibration-rotational states of diatomic molecules, Comput. Phys. Commun. 30 (1983) 101–105.

[19] F.M. Fernandez, J.F. Ogilvie, Symbolic programmes for analysis of diatomic vibration-rotational spectra, MapleTech. 5 (1998) 42–46.

[20] S.R. Langhoff, C.W. Bauschlicher, J. Partridge, Theoretical dipole moment for the $X^2\Pi$ state of NO, Chem. Phys. Lett. 223 (1994) 416–422.

[21] G. Chandraiah, P. Gillard, Absorption intensity measurements of the second overtone band of NO, Can. J. Phys. 69 (1991) 597–602.

[22] A. Goldman, L.R. Brown, W.G. Schoenfeld, M.N. Spencer, C. Chackerian, L.P. Giver, H. Dothe, C.P. Rinsland, L.H. Coudert, V. Dana, J.-Y. Mandin, NO line parameters: review of 1996 HITRAN update and new results, J. Quant. Spectrosc. Radiat. Transfer 60 (1998) 825–838.